Pergamon

*Journal of Structural Geology*, Vol. 17, No. 3, pp. 357 to 369, 1995

0191-8141/95 $9.50+0.00

0191-8141(94)00062-X

# Cleavage development within a foreland fold and thrust belt, southern Pyrenees, Spain

JAMES E. HOLL and DAVID J. ANASTASIO

Department of Earth and Environmental Sciences, 31 Williams Drive, Lehigh University, Bethlehem, PA 18015-3188, U.S.A.

(*Received* 13 *July* 1993; *accepted in revised form* 2 *May* 1994)

**Abstract**—In the southern Pyrenees lithologically distinct cleavage fronts are each parallel to bedding and dip ~20° towards the foreland. Pressure solution was the dominant mechanism of cleavage development. The mudstone cleavage front is coincident with the ~195°C paleoisotherm and is associated with a pressure solution strain of ~5%, a mechanical twin strain of ~4%, and a deviatoric stress magnitude of ~65 MPa. Illite crystallinity measurements define a geothermal gradient of 15°C $km^{-1}$ and indicate that the paleoisotherms are bedding-parallel. Deviatoric stress magnitudes, from calcite twins, were regionally constant at ~65 MPa and principal stress axes were perpendicular to cleavage. Temperature was the primary control on deformation micromechanisms and the position and orientation of the cleavage front within the foreland thrust wedge. Deformation below the cleavage front occurs predominantly by pressure solution, which in conjunction with mechanical twinning and microfracturing produces a quasi-plastic rheology. Stress magnitudes determined from mechanical twinning of carbonate grains and long-term ($10^6$–$10^{76}$ y) strain rates determined for regional folds and faults suggest an apparent macroscopic viscosity of $9.8 \times 10^{18}$ to $7.2 \times 10^{19}$ Pa s for the lower thrust wedge. Above the cleavage front temperature, pressure solution strain, total strain, and mesoscale deformation diminish. The region of the thrust wedge above the ~100°C paleoisotherm is characterized by large brittle faults with cataclastic fault zones and negligible grain-scale deformation indicating an elastico-frictional rheology.

## INTRODUCTION

Tectonic fabric development involves textural and chemical changes which result from strain and mass transfer. Within a mountain belt, the onset of cleavage is marked by a 'cleavage front', the boundary between uncleaved and cleaved rocks while the 'tectonite front' delineates the onset of a preferred crystallographic orientation (Fourmarier 1923, Fellows 1943). The tectonite and cleavage fronts are migrating interfaces which record the cumulative effects of the structural and metamorphic history of a region. The tectonite front likely records paleoisotherm geometry and has been used to infer thrust wedge geometry (e.g. Evans & Dunne 1989) however, its use necessitates abundant grain-scale measurements of crystallographic fabrics. The cleavage front is a readily observable macroscopic feature which should also record the geometry, state of finite strain, and thermal conditions of deformation. Both the tectonite and cleavage fronts are lithologically controlled (e.g. Marshak & Engelder 1985, Mitra 1987) and parameters governing the onset of crystallographic and macroscopic fabrics in various lithologies must be empirically established.

Intense study since the nineteenth century has established that low-grade fabrics are dominated by pressure solution (e.g. Plessman 1965, Trurnit 1968, Durney 1972, Rutter 1983). Prior studies have attributed the onset of cleavage to a minimum overburden of 5–7 km (e.g. Fourmarier 1923, Siddans 1977, Pique 1982, Engelder & Marshak 1985), principal extensions of >20% (e.g. Cloos 1947), temperatures exceeding ~175°C for limestones (e.g. Groshong *et al.* 1984) and ~300°C for siliciclastic rocks (e.g. Kerrich & Allison 1979, Elliott 1973, 1976), or exceeding a critical normal stress (e.g. Rutter 1983). Establishing the controls on cleavage formation will allow the cleavage front to be used much as a metamorphic isograd, indicating a particular deformation state and set of environmental conditions within an orogenic foreland.

In order to establish the controls on the cleavage front we examine the environmental and lithological controls on the development of cleavage within two south Pyrenean thrust sheets. We use geologic maps and cross-sections to determine the geometry of the cleavage front and grain-scale measurements to partition strain by deformation mechanism and determine the environmental conditions of cleavage formation. Grain size, mineralogy, and total finite strain were measured and peak temperature and deviatoric stress were estimated in regionally distributed samples. These data are used to reconstruct the syn-orogenic Pyrenean foreland and to characterize the rheological properties of the thrust wedge.

## GEOLOGIC SETTING

The Pyrenees are a result of the late Cretaceous collision of the Iberian and Eurasian plates. Collision produced a fold and thrust belt which shortened the cover sequence of northern Iberia by ~50% (Fig. 1, ECORS Pyrenees Team 1988). The cover stratigraphy in Spain includes Triassic non-marine to shallow marine

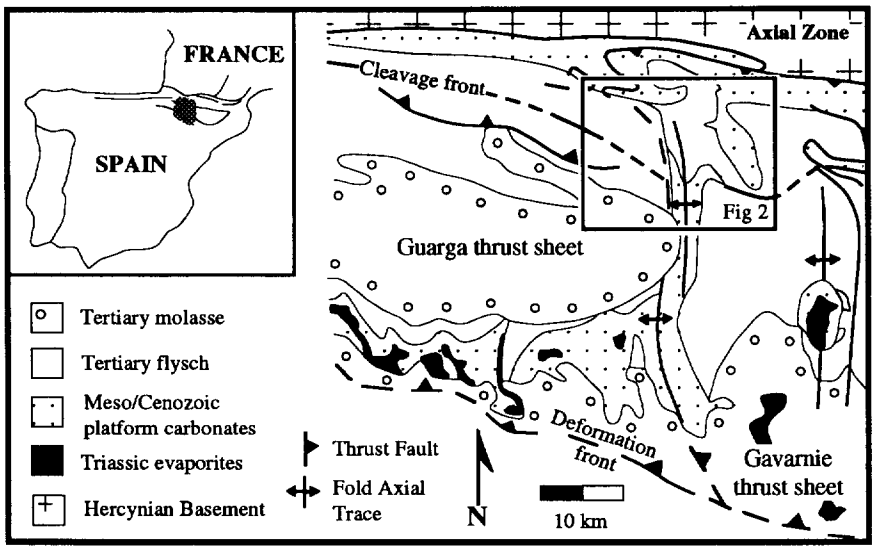


Fig. 1. Generalized geologic map of the Spanish Pyrenees. Box indicates location of Fig. 2.

clastic and carbonate rocks plus evaporites deposited during the break-up of Pangea (Mey *et al.* 1968, Mattauer & Henry 1974, Johnson & Hall 1989). Throughout the remainder of the Mesozoic, a sequence of shallow marine units were deposited prior to the onset of continental collision (Mey *et al.* 1968, Van Hoorn 1970, Mattauer & Henry 1974). The south Pyrenean foreland basin was detached and transported towards the foreland as it accumulated an average of 4000 m of Paleogene flysch while up to 1500 m of shallow marine carbonates accumulated along basin margins (Fig. 1, Rossell & Puigdefábregas 1975, Ori & Friend 1984, Johnson & Hall 1989). The onset of cleavage is studied within the flysch. As shortening continued the flysch was overlain by several kilometers of Oligocene and Miocene molasse (Puigdefábregas 1974, Friend *et al.* 1981, Mutti *et al.* 1988).

In the Boltaña region a profile of the foreland thrust wedge is exposed in the northern limb of a regional synclinorium produced by the out-of-sequence development of an antiformal stack in the axial zone (Fig. 1). Cleavage development was studied in exposures of the Guarga and Gavarnie thrust sheets (Fig. 1). The Guarga thrust sheet is bound to the north by the frontal ramp of the overlying Gavarnie thrust sheet and to the east by its oblique ramp. Both thrust sheets were transported towards S20°W. The oblique ramp of the Gavarnie thrust sheet is localized by two halotectonic-related transverse folds, the Boltaña and Anisclo anticlines (Fig. 2). During the emplacement of the Gavarnie thrust sheet, a series of meter- to kilometer-scale chevron folds developed in the Eocene flysch of the underlying Guarga thrust sheet and locally accommodate ~30% shortening. The trend of regional and mesoscale fold axes varies from N70°W in the footwall of the frontal ramp segment to north–south in the footwall of the oblique ramp (Fig. 2, Holl 1994).

Within the Boltaña region, flysch deposits consist of interbedded calcareous mudstones and sandstones in the Guarga thrust sheet and predominantly carbonate turbidites in the Garvarnie thrust sheet. Calcareous sandstones within the Guarga thrust sheet are immature and composed of poorly sorted quartz, calcite, lithic fragments, and phyllosilicate grains. Cleavage occurs in mudstones, very fine- to fine-grained sandstones (0.07–0.25 mm), and medium-grained sandstones (0.25–0.50 mm). The two most common framework minerals within the sandstones are subrounded to subangular grains of quartz (22–43%) and subrounded to rounded calcite grains (31–57%). Subrounded to rounded lithic fragments and phyllosilicate grains compose 2–28% and <1–16% of the framework grains, respectively. Accessory minerals in the sandstones include potassium feldspar, plagioclase feldspar, apatite, zircon, and opaque minerals. Carbonate-rich turbidites of the Gavarnie thrust sheet consist predominantly (>75%) of subrounded calcite grains with subsidiary quartz (~8%), phyllosilicates (~8%), and feldspars (<1%).

## CLEAVAGE AND THE CLEAVAGE FRONT

Cleavage is characterized by selvages of variable widths and lengths which anastamose around grains of quartz, calcite, and other subsidiary minerals. The selvages contain fine-grained clays, pyrite, and magnetite. Truncated and sutured quartz and calcite grain contacts, residual selvages, and quartz and calcite overgrowths suggests that pressure solution of quartz and calcite was operative. In addition, cathodoluminscence microscopy reveal abundant stable and transgranular microveins and multiple generations of carbonate overgrowths (Fig. 3). Framework carbonate grains are non-luminescent or have a bright luminescence while sparry calcite filling early extensional fractures is non-luminescent. Carbonate cement is commonly observed as a bright grain coating or is non-luminescent. The non-luminescent extensional fractures are commonly cleaved and are folded within the region. Additional generations of calcite exhibiting moderate to dull luminescence is re-

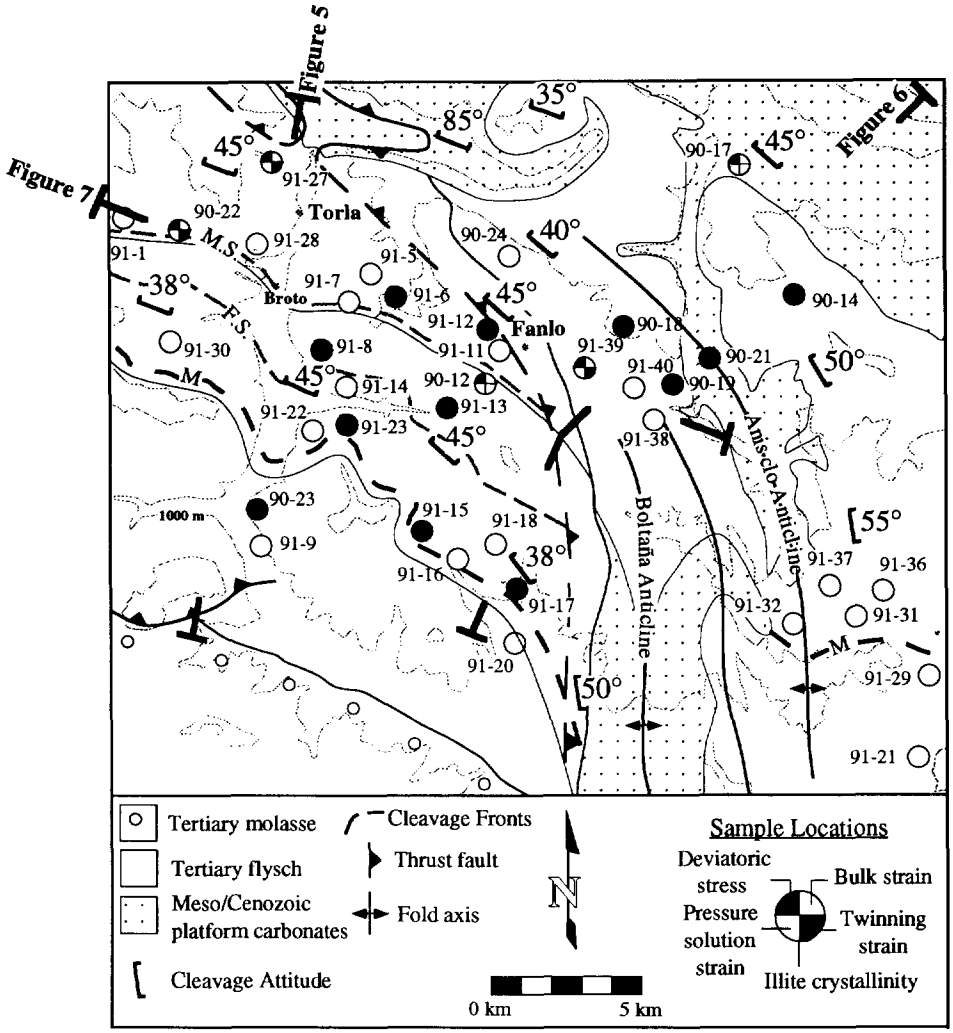


Fig. 2. Simplified geologic map of the Boltaña region. The position of the cleavage fronts for mudstones (M), fine-grained sandstones (F.S.), and medium-grained sandstones (M.S.) are indicated. The orientation of cleavage hindward of the cleavage front, major structures, principal stratigraphic units, and cross-section lines are also shown. The location of sampling sites and the type of data collected at each site are indicated, open circles represent illite crystallinity measurements only and filled circles represent samples analyzed for illite crystallinity, deviatoric stress, bulk strain, pressure solution strain and mechanical twin strain.

stricted to fibrous and non-fibrous overgrowths in the $X$-direction (where $X > Y > Z$ are principal strain axes) and filling non-fibrous syntaxial microveins which are perpendicular to cleavage strike ($YZ$ plane) and which cross-cut the folded veins. Calcite overgrowths are absent in the $Y$-direction. Mechanical twins within calcite and dolomite grains indicate that mechanical twinning was an operative deformation mechanism throughout the deformation.

The strike of cleavage within the region varies from nearly east–west in the vicinity of the frontal ramp of the Gavarnie thrust fault to north–south near the oblique ramp (Fig. 2). Cleavage is axial planar to regional and mesoscale folds and parallels the strike of the Gavarnie thrust fault. Cleavage within Eocene mudstones of the Guarga thrust sheet and carbonate-rich turbidites of the Gavarnie thrust sheet dips ~35–55°NE (Figs. 2 and 4). Cleavage is absent to poorly developed within massive Cretaceous sandstones and limestones exposed within the Gavarnie thrust sheet. Where cleavage occurs in the massive layers, it is significantly steeper than in the overlying flysch, except for a narrow zone (<20 m) within Cretaceous limestone near the base of the Gavarnie thrust sheet (Figs. 2 and 4).

Utilizing excellent exposures and available relief, cleavage fronts were mapped within Eocene flysch of the Guarga and Gavarnie thrust sheets in the Boltaña region of the south-central Pyrenees (Fig. 2). The macroscopic mudstone cleavage front represents the first appearance of cleavage within mudstones and is located ~40 km from the emergent deformation front. Cleavage fronts representing the first appearance of cleavage within very fine- to fine- and medium-grained sandstones are located stratigraphically lower and successively more hindward. We determined the attitude of cleavage fronts by direct measurements using available three-dimensional exposures and by three-point solutions. The measurements indicate that the mudstone cleavage front is bedding parallel. The cleavage fronts have an average dip of 20–25° towards the foreland in the Guarga thrust sheet and 15–20° towards the foreland in the Gavarnie thrust sheet (Figs. 2 and 4). Overall the cleavage fronts

Table 1. Kübler indices, temperature, stress, and strain data from samples located in Fig. 2

| Sample | Kübler index | Temp. °C | Stress* (Mpa) | Stress† (Mpa) | Bulk Short. (%) | Mech. Twin Short. (%) | P.S.‡ Short. (%) | P.S.§ Short. (%) |
|---|---|---|---|---|---|---|---|---|
| 90-9 | 0.20 | 230 | | | | | | |
| 90-12 | 0.41 | 209 | | | | | | |
| 90-12A | 0.41 | 209 | 67 | | | | | |
| 90-14 | 0.35 | 215 | 61 | | 25 | 4 | 21 | |
| 90-17 | 0.20 | 230 | 60 | 268 | | | | |
| 90-18 | 0.29 | 221 | 67 | 262 | 26 | 4.7 | 21.3 | 20 |
| 90-19 | 0.30 | 220 | 69 | 246 | 27 | 2 | 25 | |
| 90-21 | 0.18 | 232 | | | 26 | 4 | 22 | |
| 90-22 | 0.36 | 214 | | | | | | |
| 90-23 | 0.59 | 191 | 66 | 236 | 4 | 3.6 | 0.4 | |
| 90-24 | 0.24 | 226 | | | | | | |
| 91-1A | 0.40 | 210 | | | | | | |
| 91-1 | 0.41 | 209 | | | | | | |
| 91-5 | 0.33 | 217 | | | | | | |
| 91-6 | 0.30 | 220 | 65 | 252 | 27 | 4 | 23 | 21 |
| 91-7 | 0.59 | 191 | | | | | | |
| 91-8 | 0.47 | 203 | 67 | 245 | 17 | 5 | 12 | |
| 91-9 | 0.59 | 191 | | | | | | |
| 91-11 | 0.33 | 217 | | | | | | |
| 91-12 | 0.35 | 215 | 63 | 244 | 23 | 4.5 | 18.5 | 18 |
| 91-13 | 0.47 | 203 | 67 | 245 | 17 | 5 | 12 | |
| 91-14 | 0.51 | 199 | | | | | | |
| 91-15 | 0.59 | 191 | 62 | 249 | 9 | 3.2 | 5.8 | 5 |
| 91-16 | 0.40 | 210 | | | | | | |
| 91-17 | 0.56 | 194 | | 247 | 9 | 3.5 | 5.5 | |
| 91.18 | 0.51 | 199 | | | | | | |
| 91-20 | 0.52 | 198 | | | | | | |
| 91-21 | 0.53 | 197 | | | | | | |
| 91-22 | 0.55 | 195 | | | | | | |
| 91-23 | 0.56 | 194 | 67 | 249 | 9 | 3.2 | 5.8 | 5 |
| 91-25 | 0.28 | 222 | | | | | | |
| 91-27 | 0.33 | 217 | 62 | 246 | | 2 | | |
| 91-28 | 0.35 | 215 | | | | | | |
| 91-29 | 0.53 | 197 | | | | | | |
| 91-30 | 0.53 | 197 | | | | | | |
| 91-31 | 0.51 | 199 | | | | | | |
| 91-32 | 0.50 | 200 | | | | | | |
| 91-36 | 0.49 | 201 | | | | | | |
| 91-37 | 0.49 | 201 | | | | | | |
| 91-38 | 0.29 | 221 | | | | | | |
| 91-39 | 0.28 | 222 | 65 | 252 | | 4 | | |
| 91-40 | 0.33 | 217 | | | | | | |

*Jamison and Spang's (1976) technique.
†Rowe and Rutter's (1990) technique.
‡Calculated by subtracting twin shortening from bulk shortening.
§Measured using cathodoluminscence microscopy.

are distributed across an ~9 km wide zone in map view which exposes an ~3 km thick stratigraphic section where cleavage in each lithology progressively developed at different depths within the thrust wedge (Fig. 2).

The intensity and onset of cleavage varies as a function of structural position, lithology, and position within the thrust wedge. Generally, cleavage becomes more closely spaced in stratigraphically lower positions which corresponds to increasing distance north of the cleavage front. On an outcrop scale, the selvages are more continuous and more closely spaced in finer grained rocks and in mesoscale fold hinges than in coarser units or on fold limbs. For comparative purposes the intensity of cleavage is described on the basis of field measurements of selvage spacing in backlimb positions, using the classification scheme of Alvarez *et al.* (1978). Cleavage spacing within mudstones ranges from weakly developed (>7 cm spacing) adjacent to the cleavage front to very strongly developed (2–3 mm spacing) 9 km hindward of the cleavage front in map view (~3 km stratigraphically lower). The onset of cleavage in very fine- to fine-grained sandstones occurs ~3 km hindward of the mudstone cleavage front in map view and ~1 km stratigraphically below the mudstone cleavage front. Cleavage spacing within the fine sandstones is strongly developed 9 km hindward of the mudstone cleavage front. Within the area medium-grained sandstones possess a spaced cleavage which ranges from weakly developed ~5 km hindward of and ~1.7 km below the mudstone cleavage front to moderately well-developed (3–5 cm spacing), 9 km hindward.

## DEFORMATION CONDITIONS

### *Deviatoric stress*

Mechanically twinned carbonate grains within samples collected along a north–south transect across the Guarga thrust sheet and a northeast–southwest

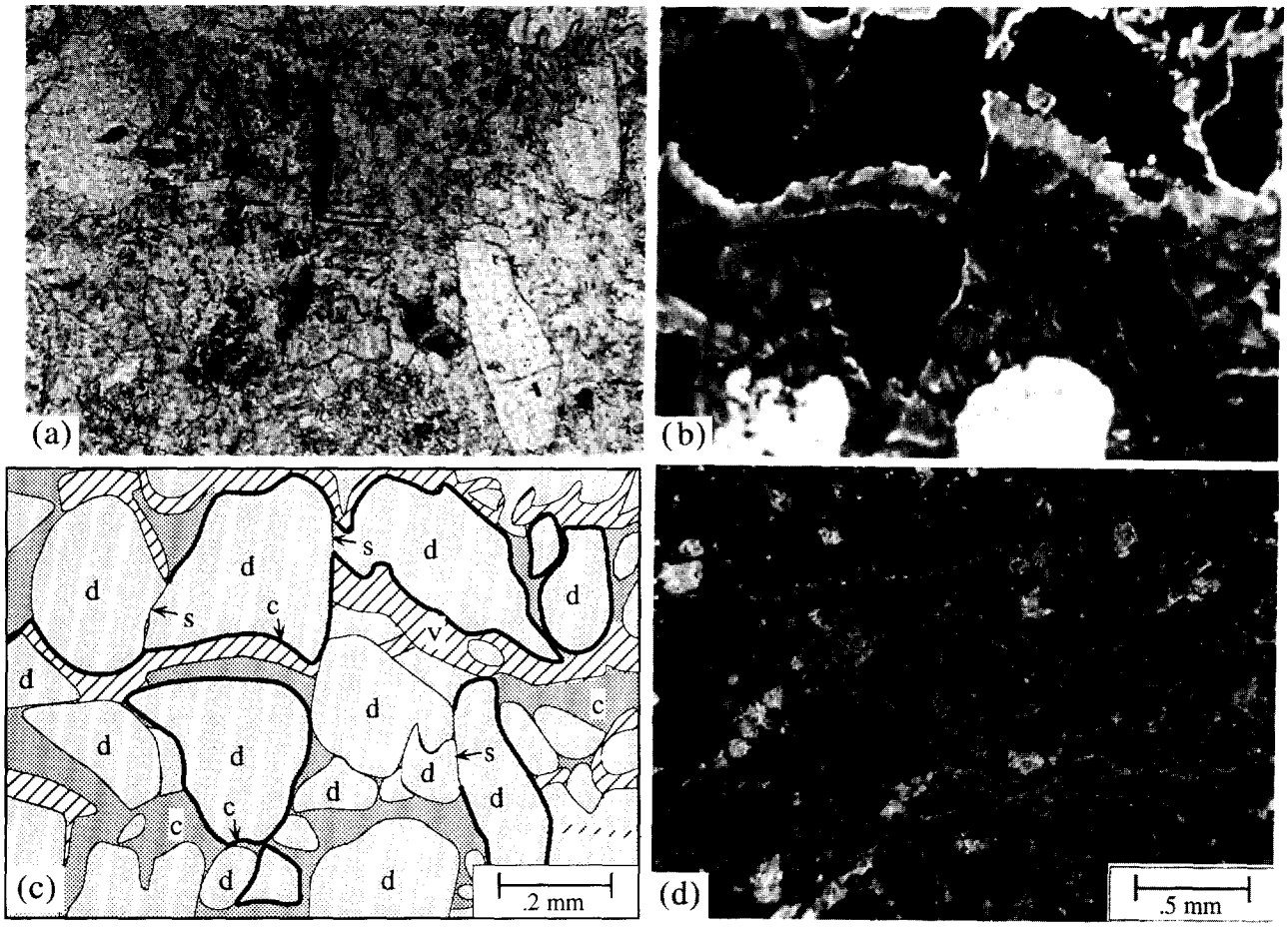


Fig. 3. (a) & (b) Photomicrographs of sample 91-6 taken in plane light (a) and cathodoluminescence (b). Accompanying sketch (c) shows the position of detrital grains—d, carbonate cement—c, veins and overgrowths—v, and sutured grain contacts—s. (d) Photomicrograph of sample 91-6 taken in cathodoluminescence showing calcite filled microveins. The total strain for this sample is 1.7 (~27% shortening in the Z-direction), the mechanical twin strain is ~4%, and the pressure solution strain averaged across the thin section is ~21%.

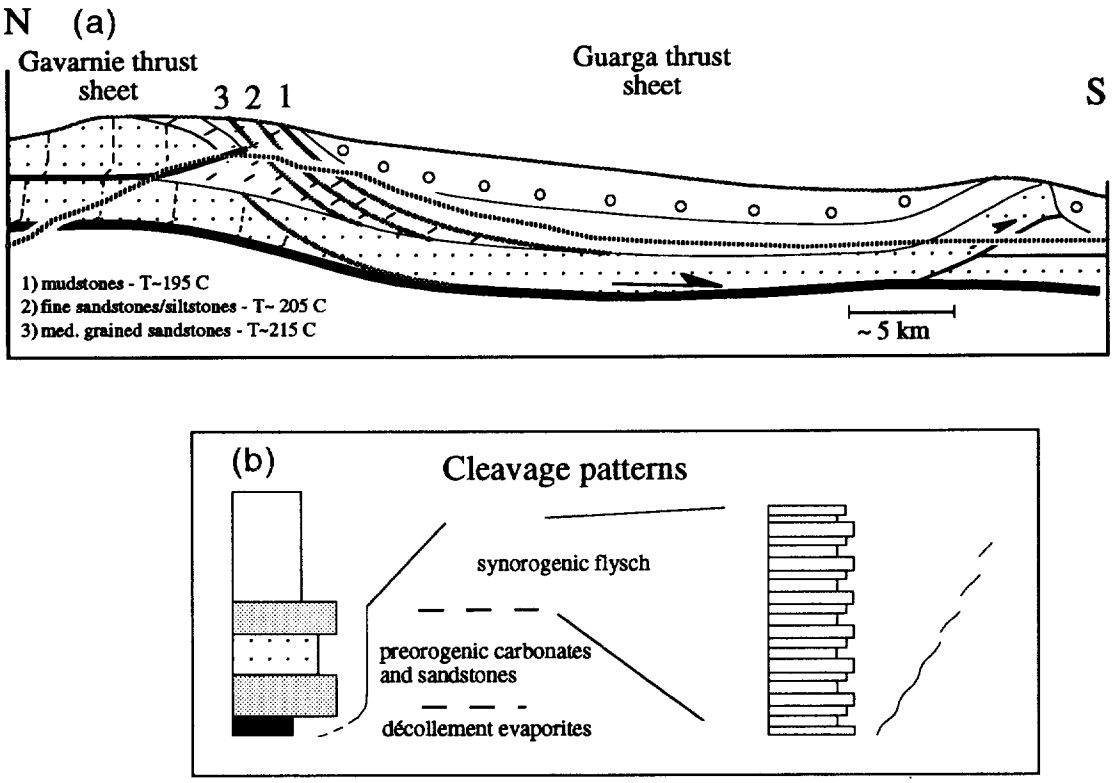


Fig. 4. (a) Schematic north–south cross-section through the southern Pyrenees showing the orientation of cleavage and the position and orientation of the cleavage fronts for various lithologies. (b) Composite cleavage trajectory for south Pyrenean thrust sheets.

oriented transect across the oblique ramp of the Gavarnie thrust sheet were used to estimate maximum deviatoric stress magnitudes (Table 1; Figs. 2, 5 and 6). Twin density and the percentage of carbonate grains with one, two, or three twin sets were measured using universal- and flat-stage microscopy. The use of carbonate minerals as a paleopiezometer is based on the observation that single crystals of carbonate oriented favorably for slip will twin when the magnitude of deviatoric stress reaches the yield stress. Estimates of yield stresses range from 10 MPa for calcite to as high as 60–120 MPa for dolomite (Tullis 1980). Samples from the southern Pyrenees commonly contain both twinned dolomite and calcite.

Jamison & Spang (1976) used the percentage of calcite and dolomite grains in aggregates with one, two, and three twin sets to estimate deviatoric stress and found that for strains less than 3–4%, the calculated stresses closely matched experimental calibrations. Point counts of samples from this study reveal ~70% of the calcite grains contain at least one set of mechanical twin lamellae, ~20% of the grains contain two or more sets, and <1% contain three sets of twin lamellae. The lack of calcite grains with three sets of mechanical twins suggests a maximum deviatoric stress magnitude of ~70 MPa (Jamison & Spang 1976). The measured frequency of calcite grains twinned by one and two sets of lamellae suggests that deviatoric stress magnitudes were nearly constant across the studied region and ranged between 60 and 69 MPa (Figs. 5 and 6).

Deviatoric stresses were also calculated using the approach of Rowe & Rutter (1990) using point count data with universal-stage measurements of twin density. Deviatoric stresses were nearly constant across the region, ranging between 236 and 268 MPa (Table 1; Figs. 5 and 6). The total variance of the data is within the standard error of the technique, ~43 MPa, measured experimentally by Rowe & Rutter (1990).

Turner Dynamic Analyses (Turner 1953) were used to determine the orientation of the principal stress axes. Results of the analyses indicate that the principal compressive stress axes had a subhorizontal plunge and a trend perpendicular to cleavage varying from N20°E to N90°E. The intermediate principal compressive stress direction was subhorizontal and the least compressive stress direction was vertical.

*Finite strain/strain partitioning*

Finite strain was measured in a cleavage-parallel plane and perpendicular to the intersection of bedding and cleavage of fine and medium-grained sandstone samples collected along the transects. Bulk finite strain was measured on thin sections by the enhanced normalized Fry method (Erslev 1988, Erslev & Ge 1990). Object-pair selection factors were chosen so that analyses included 60 touching pairs for every 100 objects and generally ranged between 1.0 and 1.2. Cathodoluminescence observations reveal no tectonic overgrowths in the $Y$-direction indicating that the deformation was plane strain ($\sqrt{\lambda_y} = 1$). In order to compare total strains to strain partitioning results, $XZ$ axial ratios calculated by the normalized Fry method were converted to percent-

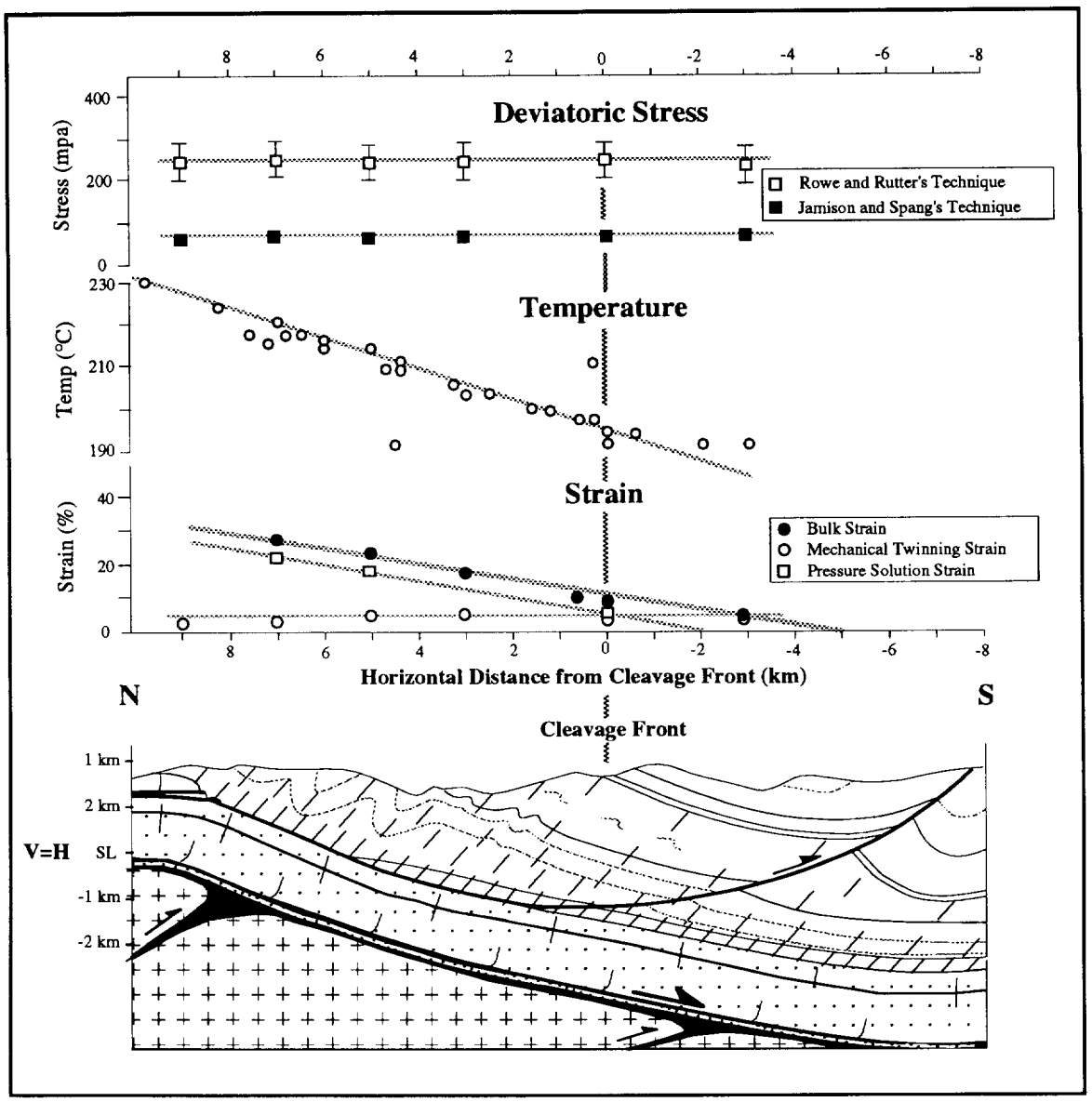


Fig. 5. North–south oriented cross-section showing the position of the mudstone cleavage front, see Fig. 2 for location. The orientation and intensity of cleavage hindward of the cleavage front is schematically depicted. Also shown are graphs of bulk strains, mechanical twinning strains, pressure solution strains, deformation temperature, and deviatoric stress magnitudes vs distance from the mudstone cleavage front.

age shortening in the $Z$-direction by assuming that the deformation was constant volume. In general, the $Z$ axis of the strain ellipse is perpendicular to the plane of cleavage. Along the north–south, traverse total shortening the $Z$-direction increases linearly from <5% 2 km forward of the cleavage front to ~30%, ~7.5 km hindward of the cleavage front (Fig. 5). A similar relationship was observed along the northeast–southwest traverse, where total strains increased from ~5%, 1 km south of the cleavage front, to >30%, in the Gavarnie thrust sheet (Fig. 6). Observed increases in bulk strain are consistent with patterns observed in many other orogens and result from increasing proximity to the Gavarnie thrust fault and to the hinterland of the mountain belt (e.g. Cloos 1947).

An inverse linear relationship was observed between bulk strains and cleavage spacing for fine- and medium-grained sandstones. The first appearance of a weakly-developed cleavage within fine- and medium-grained sandstones is associated with a principal shortening of 15–20%. Cleavage within the fine-grained sandstones is strongly developed at a principal shortening of 25–30%. Medium-grained sandstones were locally strongly cleaved in fold hinges but does not display a pervasive cleavage in the region. Cleavage within coarse-grained sandstones was only locally present in fold hinges.

Total finite strain was partitioned into the three competing deformation mechanisms: (1) mechanical twinning, and (2) pressure solution coupled with (3) microfracturing. Mechanical twinning strains were measured using Groshong's (1972) calcite strain gauge on calcite grains from within the matrix and within pre- and syn-cleavage extensional fractures. Twinning strains are low and nearly constant along the traverses ranging between

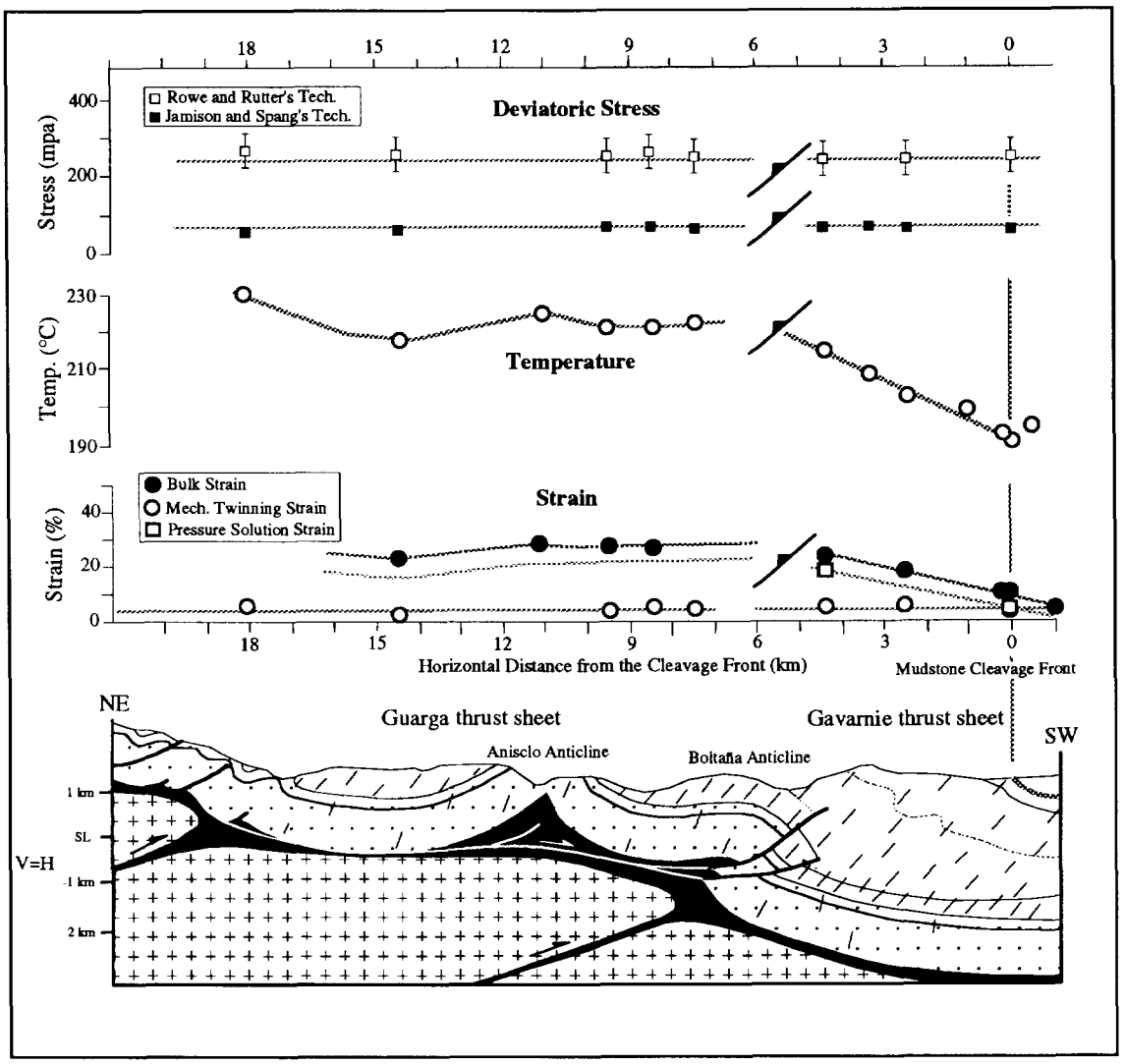


Fig. 6. Northeast–southwest oriented cross-section showing the position of the mudstone cleavage front, see Fig. 2 for location. The orientation and intensity of cleavage hindward of the cleavage front is schematically represented. Also shown are graphs of bulk strains, mechanical twinning strains, pressure solution strains, deformation temperature, and deviatoric stress magnitudes vs distance from the mudstone cleavage front.

2–5% and averaging 4% (Table 1; Figs. 5 and 6). The maximum shortening direction is perpendicular to cleavage for all samples hindward of the cleavage front. Pressure solution strain for each sample was calculated by subtracting the mechanical twinning strain from the bulk strain calculated from the normalized Fry axial ratios. Calculated values of pressure solution strain were checked by directly measuring overgrowths and veins ($\sqrt{\lambda_x}$) in cathodoluminescence. The percent extension recorded by microveins and overgrowths was determined along multiple traverses across several photomicrographs for each of five samples (Fig. 3). The measured extension values were nearly equal to the values calculated using the difference between bulk and mechanical twin strains (Figs. 5 and 6). The magnitude of the pressure solution strains mimicked the observed increase in total strains north of the mudstone cleavage front. Pressure solution strains are ~0%, 2 km forward of the cleavage front, 5% at the cleavage front, and ~25%, ~7.5 km hindward of the cleavage front.

*Peak temperature*

Peak metamorphic temperatures were estimated throughout the Boltaña region using illite crystallinity. The crystallinity of illite is quantified by measuring the basal (001) illite 10 Å peak at half-intensity on an X-ray diffractogram (Kübler 1967, Kisch 1987). Temperature is thought to be the major variable affecting illite crystallinity, however, total strain, strain rate, and the amount of pressure solution may also affect measured values (e.g. Nyk 1985, Marshak & Engelder 1985, Kreutzberger & Peacor 1988). In order to evaluate the effects of total strain and pressure solution strain on illite crystallinity; samples were analyzed around a mesoscale fold. The test revealed a variance of illite crystallinity around the fold of <1% (0.001° $2\theta$), associated with a 20% difference in total shortening measured by the Fry method and a 15% difference in pressure solution shortening. The observed variation is within the standard error of the technique suggesting that temperature and

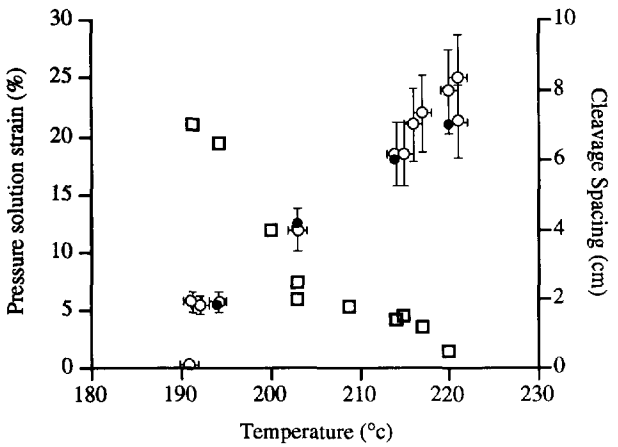


Fig. 7. Graph of temperature determined from illite crystallinity vs cleavage spacing (squares) and the pressure solution component of strain determined by subtracting the mechanical twinning strain from the bulk strain (open circles) and using cathodoluminescence microscopy (filled circles).

not strain is the primary control on variations in illite crystallinity within the region. While not a precise geothermometer illite crystallinity is an indicator of approximate peak temperatures and a guide to relative temperature variations providing an accurate means of assessing the thermal structure of the south Pyrenean thrust wedge.

Samples were prepared following the recommendations of Kisch (1991). Illite crystallinity was determined from the <2 $\mu$m fraction of 42 samples collected across the region. Regionally, Kübler indices varied from ~0.56° to 0.35° 2$\theta$ (Table 1). Paleotemperatures estimated from Kübler indices vary from ~190°C to >230°C over ~3 km of stratigraphic section, a gradient of ~15°C km$^{-1}$. Paleoisotherms inferred from the illite crystallinity data are approximately parallel to the cleavage fronts and bedding. The mudstone cleavage front correlates to the ~195° paleoisotherm (Figs. 5 and 6). The increase in Kübler indices (increasing temperature) is linearly correlated to the decrease in cleavage spacing (Fig. 7). A strike-parallel cross-section of paleoisotherm surfaces within the Guarga thrust sheet shows that they are offset by the Gavarnie thrust fault (Fig. 8).

As an additional constraint on the thermal structure of the thrust wedge we use vitrinite reflectance values of 0.42 and 0.40 in Cretaceous shales from the leading edge of the Guarga thrust sheet exposed in the External Sierra. As with illite crystallinity the reflectivity of vitrinite is likely dependent on both time and temperature (e.g. Middleton 1982). Kinetic models (e.g. Bostick 1979, Middleton 1982) and field studies (e.g. Barker 1991) suggest, however, that for burial histories characterized by uniform heating rates maximum temperature is the primary factor controlling vitrinite reflectance (Johnsson *et al.* 1993). Using the correlation of Barker (1988) we estimate peak temperatures of 53–58°C at the level of the Cretaceous in the toe of the emergent thrust system.

## DISCUSSION

### *Mechanisms of cleavage development*

Data collected within the southern Pyrenees allows determination of the principal mechanisms of cleavage development and complete characterization of cleavage fronts for a variety of lithologies. The presence of sutured grain contacts, fibrous calcite overgrowths, microveins, clay-rich selvages, and direct measurements of pressure solution strain indicates that pressure solution was the dominant mechanism of cleavage development. The lack of recrystallized grains and subgrains suggests that dislocation creep was not a significant mechanism of deformation within these rocks. Given the low deformation temperatures, grain boundary sliding was unlikely except as necessary to accommodate other active deformation mechanisms (Crussard & Tamhanker 1958, Mitra 1976).

The lack of overgrowths in the $Y$-direction and the coincidence of pressure solution strain measured by subtracting the mechanical twinning strain from the bulk strain and direct measurement of $\sqrt{\lambda_x}$ from microviens and overgrowths requires that any volume change was isotropic on the thin section scale. The presence of mantling overgrowths in the $X$-direction and restriction of dissolution textures to the $Z$-direction is inconsistent with isotropic volume loss and suggests that mass transfer associated with cleavage formation was locally volume constant. The strain balance indicates transgranular pressure solution and veining occurred simultaneously. Unstable fractures within south Pyrenean turbidites became material sinks and mass transfer conduits for calcite locally diffused from the adjacent wallrock. Mechanically twinned calcite within syn-cleavage microveins suggests locally simultaneous twinning and pressure solution.

### *The cleavage front*

Previous work suggests that the dominant variables controlling pressure solution are temperature and deviatoric stress magnitudes. Deviatoric stress magnitudes were remarkably consistent regionally but estimates vary depending on the technique used. Ferrill (1991) has recently shown that calcite twin width and density is dependent on temperature. Deformation of carbonate minerals at temperatures under ~150°–200°C is accommodated by numerous thin twins while deformation at temperatures >200°C results in fewer thick twins. Rowe & Rutter's (1990) technique was calibrated with experiments run predominantly at temperatures >400°C, while Jamison & Spang's (1976) technique is most useful in rocks deformed weakly at low temperatures (<200°C, Burkhard 1993). Deformation temperatures in the southern Pyrenees are low, therefore, Jamison & Spang's (1976) technique is considered the more accurate method of determining paleostress values for this study. Constant deviatoric stress magnitudes during cleavage development permit the assessment of the

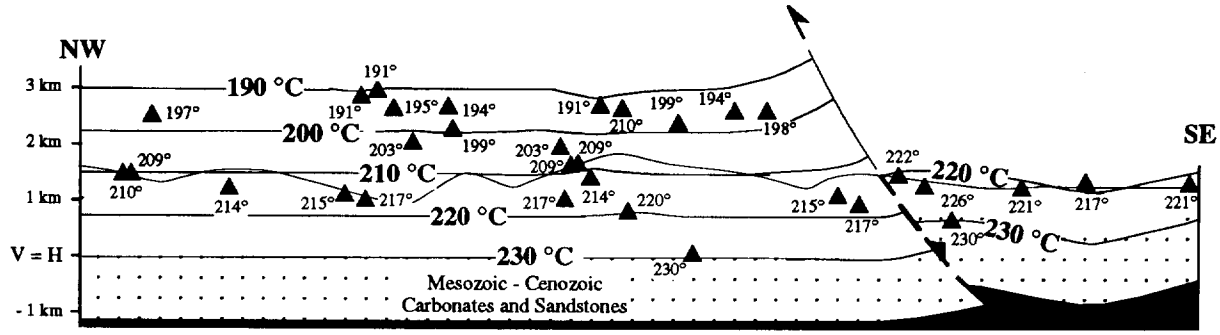


Fig. 8. East–west oriented cross-section, see Fig. 2 for location. Filled triangles indicate temperature data projected into the section plane from the north and south. The orientation and position of paleoisotherms in the Gavarnie and Guarga thrust sheets are indicated.

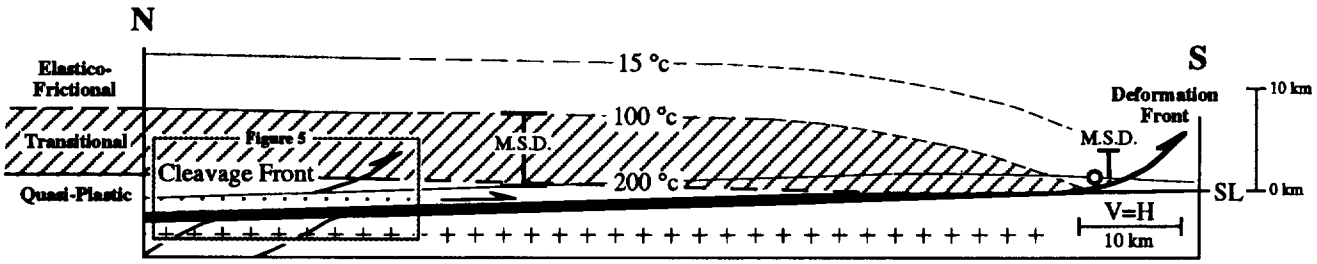


Fig. 9. Generalized palinspastic reconstruction of the Guarga thrust sheet in the southern Pyrenees. Paleoisotherms and cleavage front position shown prior to basement imbrication, open circle represents vitrinite sample location (53–58°C) from the External Sierras. M.S.D. = the maximum preserved synorogenic deposits. The location of Fig. 5 is also indicated.

effects of temperature on cleavage development and the position and attitude of the cleavage front.

The parallelism of the cleavage front with a paleoisotherm surface and the linear correlation of pressure solution strain to temperature and cleavage intensity, indicates that cleavage intensity and the position and orientation of the cleavage front in the southern Pyrenees was thermally controlled. Bedding-parallel paleoisotherms suggest that peak temperatures record maximum burial depths. The piggyback basin, hanging wall flat on footwall flat geometry, and likely long duration of deformation ($\sim 10^6$–$10^7$ y, Anastasio 1992, Burbank *et al.* 1992, Deramond *et al.* 1993) requires that maximum burial (peak temperatures) coincides with thrusting and cleavage development. The orthogonal relationship between cleavage and the maximum stress direction indicates that while the position of the cleavage front was thermally controlled, the orientation of cleavage behind the front was dependent on the orientation of the maximum principal compressive stress.

*Implications for thrust belt development*

Axial planar cleavage in fault-bend and décollement folds and a shallowing of cleavage dip from ~90° to ~50° near the base of the Gavarnie thrust sheet suggests that cleavage development and thrust sheet emplacement were coeval. Because cleavage fronts within the southern Pyrenees developed during thrusting and delineate foreland paleoisotherms, they can be used with estimates of the geothermal gradient to estimate the position of the synorogenic surface. In order to determine the attitude of isotherms and the position of the synorogenic surface later basement faults were restored along the north–south section through the Guarga thrust sheet. The generalized reconstruction was accomplished by restoring the Hercynian basement beneath the Guarga thrust sheet to its pre-imbrication dip of ~2° (ECORS Pyrenees Team 1988) and by restoration of later imbrication within the toe of the thrust wedge (Fig. 9). Using the restored position of the paleoisotherms, the calculated geothermal gradient of ~15°C $km^{-1}$, and assuming an average surface temperature of 15°C, we reconstructed the position of the synorogenic ground surface to ~11 km above the cleavage front. Measurement of the aggregate thickness of syn-orogenic deposits preserved within the south Pyrenean foreland basins suggests a maximum depositional thickness of ~7 km above the cleavage front. Possible reasons for discrepancies in the position of the synorogenic surface include: (1) unrecognized erosion of synorogenic cover (unlikely); (2) the narrow stratigraphic interval over which the geothermal gradient was calculated; (3) advective heat transport by fluid flow; (4) the kinetic dependence of illite crystallinity on time at temperature; and most likely (5) structural thickening of syn-tectonic strata within the deforming piggyback basin (e.g. Puigdefábregas 1975, Labaume *et al.* 1985).

Thermal modelling by Barr & Dahlen (1991) indicate that shallow foreland isotherms (<300°C) are subparallel to the topographic surface. As a proxy for isotherm geometry, cleavage fronts can provide a record

of the attitude of the top of the deforming thrust wedge. Figure 9 indicates that shallow isotherms and the synorogenic surface in the southern Pyrenees had a dip of <2° towards the foreland prior to basement imbrication. With a basal décollement dip of 2° the taper angle of the thrust wedge was 3°–4°.

The strain partitioning studies allow a rheological assessment of the south Pyrenean thrust wedge (Fig. 9). Orogens have been viewed as consisting of an upper elastico-frictional regime and lower quasi-plastic regime (e.g. Sibson 1977, Wojtal & Mitra 1988). Below the cleavage front (~195°C) pervasive pressure solution coupled with microfracturing leading to cleavage formation plus mechanical twinning occurs at a grain-scale while abundant faults and folds characterizes deformation at larger scales. The presence of shear fibers on regional and mesoscale fault surfaces indicates that the faults moved by pressure solution slip (Elliott 1976). Shear fibres on mechanically active bedding planes in folds and the development of axial planar disjunctive cleavage suggests that folding was also accommodated by pressure solution. The portion of the wedge below the cleavage front can therefore be characterized as quasi-plastic. The portion of the thrust wedge between the cleavage front and the ~100°C paleoisotherm contains little penetrative pressure solution and mechanical twin strain and fewer mesoscale faults that record pressure solution slip. This region is transitional in rheology between the lower quasi-plastic wedge and the upper (<100°C) portion of the thrust wedge which is characterized by emergent imbricates with large brittle zones of 4–12 m thick protocataclasites, some mesoscale pressure solution slip faults, and a near absence of grain-scale strain except minor mechanical twinning. The upper region of the wedge is best characterized by an elastico-frictional rheology.

Within the quasi-plastic regime deformation was dominated by pressure solution on a wide range of scales. Pressure solution is known to produce a linear viscous rheology with the effective viscosity equal to the ratio of stress to strain rate (Jaeger & Cook 1976). Because mechanical twinning and pressure solution were coeval, deviatoric stress magnitudes determined from carbonate twins reflect maximum stresses coincident with pressure solution. Strain rates have been previously estimated on temporal scales from $10^6$–$10^7$ y and spatial scales from $10^{-1}$–$10^1$ km. Holl & Anastasio (1993) and DePaor & Anastasio (1987) used balanced cross-sections and/or biostratigraphic magnetostratigraphic age constraints to calculate time averaged strain rate of $0.9 \times 10^{-15}$ s$^{-1}$ for thrust sheet motion and regional-scale folding. Burbank *et al.* (1992) used magnetostratigraphies to reconstruct the history of motion for several eastern Pyrenees thrust sheets and report average strain rates of $2–4 \times 10^{-15}$ s$^{-1}$. The strain rate estimates do not vary much over $10^6$–$10^7$ y averages. Using the estimates of strain rate and deviatoric stress we calculate an effective macroscopic viscosity of $9.8 \times 10^{18}$ to $7.2 \times 10^{19}$ Pa s for the lower portion of the south Pyrenean thrust wedge.

## CONCLUSIONS

Within the southern Pyrenees, a series of cleavage fronts define the boundary between cleaved and uncleaved mudstones, fine-grained sandstones, and medium-grained sandstones. The cleavage fronts are each bedding-parallel and distributed across a 10 km wide zone in map view (~3 km of stratigraphic section), located ~40 km from the deformation front, in which cleavage progressively developed within the thrust wedge. Analyses of regionally distributed samples indicates that the mudstone cleavage front is coincident with the 195°C paleoisotherm and is associated with a mechanical twinning strain of ~4%, a pressure solution strain of ~5%, and a deviatoric stress of ~65 MPa. Petrographic and cathodoluminescence microscopy of the samples indicate that mechanical twinning, microfracturing, and pressure solution were operative during emplacement of south Pyrenean thrust sheets.

Measurement of the illite crystallinity in samples collected regionally delineates a geothermal gradient of 15°C km$^{-1}$ and indicates that the paleoisotherms are bedding-parallel. The parallelism of cleavage fronts and paleoisotherms and the linear correlation of pressure solution strains to cleavage intensity and temperature indicates that temperature was the primary control on deformation mechanism partitioning within the thrust wedge. Restoration of the south Pyrenean paleoisotherms, which provide an estimate of the orientation of the synorogenic surface, dipped <2° towards the foreland prior to basement imbrication. Below the cleavage front (~195°C) the thrust wedge can be characterized by a quasi-plastic rheology and above a broad transitional region between the cleavage front and the ~100°C isotherm the wedge is best modelled with an elastico-frictional rheology. Over a wide range of scales, deformation within the quasi-plastic region of the wedge was dominated by pressure solution. Using measured deviatoric stress magnitudes and published strain rates values, a macroscopic effective viscosity of $9.8 \times 10^{18}$ to $7.2 \times 10^{19}$ Pa s is predicted for the lower portion of the south Pyrenean thrust wedge.

*Acknowledgements*—Research completed as part of Holl's Ph.D. dissertation at Lehigh University. Funded by National Science Foundation grant EAR-8816335 awarded to Anastasio and by grants to Holl from the American Association of Petroleum Geologists, Sigma Xi, and the Geological Society of America. Vitrinite reflectance data courtesy of BP Petroleum Development of Spain, S.A. We thank C. Hedlund for field assistance; B. Ricker for developing the photomicrographs; dissertation committee members T. Byrne, K. Kodama, and A. Meltzer; and E. Erslev, J. Evans, and an anonymous journal reviewer for constructive reviews of the manuscript.

## REFERENCES

Alvarez, W., Engelder, T. & Geiser, P. A. 1978. Classification of solution cleavage in pelagic limestones. *Geology* **6**, 263–266.

Barker, C. E. 1988. Geothermics of petroleum systems: implications of the stabilization of kerogen thermal maturation after a geologically brief heating duration at peak temperature. In: *Petroleum Systems of the United States* (edited by Magoon, L. B.). *U.S. Geol. Surv. Bull.* **1870**, 26–29.

Barker, C. E. 1991. Implications for organic maturation studies of evidence for a geologically rapid increase and stabilization of vitrinite reflectance at peak temperature: Cerro Prieto geothermal system, Mexico. *Bull. Am. Ass. Petrol. Geol.* **75**, 1852–1863.

Barr, T. D. & Dahlen, F. A. 1991. Brittle frictional mountain building 3: low grade metamorphism. *J. geophys. Res.* **96**, 10319–10338.

Bostick, N. H. 1979. Microscopic measurement of the level of catagenesis of solid organic matter in sedimentary rocks to aid exploration for petroleum and to determine former burial temperatures—a review. In: *Aspects of Diagenesis* (edited by Scholle, P. A. & Schluger, P. R.). *Spec. Publ. Soc. Econ. Paleont. & Mineral.* **26**, 17–44.

Burbank. D. W., Verges, J., Muñoz, J. A. & Bentham, P. 1992. Coeval hindward- and forward-imbricating thrusting in the central southern Pyrenees, Spain: timing and rates of shortening and deposition. *Bull. geol. Soc. Am.* **104**, 3–17.

Burkhard, M. 1993. Calcite twins, their geometry, appearance and significance as stress–strain markers and indicators of tectonic regime: a review. *J. Struct. Geol.* **15**, 351–368.

Cloos, E. 1947. Oolite deformation in the South Mountain fold, Maryland. *Bull. geol. Soc. Am.* **58**, 843–918.

Crussard, C. & Tamhanker, R. 1958. High temperature diffusion of steels: a study of equicohesion, activation energies, and structural modification. *Trans. Am. Instn. Min. Engrs* **212**, 718–730.

DePaor, D. M. & Anastasio, D. J. 1987. The Spanish External Sierra: a case history in the advance and retreat of mountains. *National Geographic Research* **3**, 199–209.

Deramond, J., Souquet, P., Fondecare-Wallez, M. & Specht, M. 1993. Relationships between thrust tectonics and sequence stratigraphy surfaces in foredeeps: model and examples from the Pyrenees (Cretaceous–Eocene, France, Spain). In: *Tectonics and Seismic Sequence Stratigraphy* (edited by Williams, G. D. & Dobb, A.). *Spec. Publ. geol. Soc.* **71**, 193–219.

Durney, D. W. 1972. Solution-transfer, an important geological deformation mechanism. *Nature* **235**, 315–317.

ECORS Pyrenees Team. 1988. Deep reflection seismic survey across an entire orogenic belt, the ECORS Pyrenees profile. *Nature* **331**, 508–511.

Elliott, D. 1973. Diffusion flow laws in metamorphic rocks. *Bull. geol. Soc. Am.* **84**, 2645–2664.

Elliott, D. 1976. The energy balance and deformation mechanisms of thrust sheets. *Phil. Trans. R. Soc.* **283**, 289–312.

Engelder, J. T. & Marshak, S. 1985. Disjunctive cleavage formed at shallow depths in sedimentary rocks. *J. Struct. Geol.* **7**, 327–343.

Erslev, E. A. 1988. Normalized center-to-center strain analysis of packed aggregates. *J. Struct. Geol.* **10**, 201–209.

Erslev, E. A. & Ge, H. 1990. Least-squares center-to-center and mean object ellipse fabric analysis. *J. Struct. Geol.* **12**, 1047–1059.

Evans, M. A. & Dunne, W. M. 1989. Geometry of a foreland tectonite front. *Geol. Soc. Am. Abst. w. Prog.* **21**, A67.

Fellows, R. E. 1943. Recrystallization and flowage in Appalachian quartzite. *Bull. geol. Soc. Am.* **54**, 1399–1432.

Ferrill, D. A. 1991. Calcite twin widths and intensities as metamorphic indicators in natural low-temperature deformation of limestone. *J. Struct. Geol.* **13**, 667–675.

Fourmarier, P. 1923. De L'importance de la Charge dans le Developpement du Clivage Schisteux. *Bull. Acad. R. Belgique, Cl. Sci.* **5**, 454.

Friend, P. F., Marzo, M., Nijman, E. & Puigdefábregas, C. 1981. Fluvial sedimentation in the Tertiary South Pyrenean and Ebro basins, Spain. In: *Field Guides to Modern and Ancient Fluvial Systems in Britain and Spain* (edited by Elliot, T.). University of Keele, Chapter 4, 4.1–4.50.

Groshong, R. H. 1972. Strain calculated from twinning in calcite. *Bull. geol. Soc. Am.* **83**, 2025–2038.

Groshong, R. H., Pfiffner, O. A. & Pringle, L. R. 1984. Strain partitioning in the Helvetic thrust belt of eastern Switzerland from the leading edge to the internal zone. *J. Struct. Geol.* **6**, 5–18.

Holl, J. E. & Anastasio, D. J. 1993. Paleomagnetically derived folding rates southern Pyrenees, Spain. *Geology* **21**, 271–274.

Holl, J. E. 1994. Foreland Deformation Processes, southern Pyrences, Spain. Unpublished Ph.D. Dissertation. Lehigh University.

Jaeger, J. C. & Cook, N. G. W. 1976. *Fundamentals of Rock Mechanics*. Wiley, New York.

Jamison, W. R. & Spang, J. H. 1976. Use of calcite in lamellae to infer differential stress. *Bull. geol. Soc. Am.* **87**, 878–872.

Johnson, J. A. & Hall, C. A. 1989. The structural and sedimentary evolution of the cretaceous North Pyrenean Basin, southern France. *Bull. geol. Soc. Am.* **101**, 231–247.

Johnsson, M. J., Howell, D. G. & Bird K. J. 1993. Thermal maturity patterns in Alaska: implications for tectonic evolution and hydrocarbon potential. *Bull. Am. Ass. Petrol. Geol.* **77**, 1874–1903.

Kerrich, R. & Allison, I. 1979. Flow mechanisms of rocks: microscopic and mesoscopic structures and their relation to physical conditions of deformation in the crust. *Geoscience Can.* **5**, 109–118.

Kisch, H. J. 1987. Correlation between indicators of very low-grade metamorphism. In: *Low Temperature Metamorphism* (edited by Frey, M.). Blackie & Son Ltd, 9–57.

Kisch, H. J. 1991. Illite crystallinity: recommendations on sample preparation, X-ray diffraction settings, and interlaboratory samples. *J. Meta. Geol.* **9**, 665–670.

Kreutzberger, M. E. & Peacor, D. R. 1988. Behavior of illite and chlorite during pressure solution of shaly limestone of the Kalkberg Formation, Catskill, New York. *J. Struct. Geol.* **10**, 803–811.

Kübler, B. 1967. La cristallinite de l'illite et les zones tout a fait superieures du metamorphisme. In: Etages tectoniques. A la Baconniere, Neuchatel (Suisse), 105–121.

Labaume, P., Séguret, M. & Seyve, C. 1985. Evolution of a turbiditic foreland basin and analogy with an accretionary prism: example of the Eocene south-Pyrenean basin. *Tectonics* **4**, 661–685.

Marshak, S. & Engelder, T. 1985. Development of cleavage in limestones of a fold-thrust belt in New York. *J. Struct. Geol.* **7**, 345–359.

Mattauer, M. & Henry, J. 1974. The Pyrenees. In: *Mesozoic–Cenozoic Orogenic Belts; Data for Orogenic Studies. Special Publication* 4 (edited by Spencer, A. M.). Geological Society of London. Scottish Academic Press.

Mey, P. H. W., Nagtegaal, P. J. C., Robert, K. J. & Hartevelt, J. A. A. 1968. Lithostratigraphic subdivision of post-Hercynian deposits in the south central Pyrenees, Spain. *Leid. geol. Meded.* **41**, 221–228.

Middleton, M. F. 1982. Tectonic history from vitrinite reflectance Geophys. *J. Royal Astron. Soc.* **68**, 121–132.

Mitra, S. 1976. A quantitative study of deformation mechanisms and finite strain in quartzite. *Contr. Miner. Petrol.* **59**, 203–226.

Mitra, S. 1987. Regional variations in deformation mechanisms and structural styles in the central Appalachian orogenic belt. *Bull. geol. Soc. Am.* **98**, 569–590.

Mutti, E., Séguret, M. & Sgavetti. 1988. Sedimentation and deformation in the Tertiary sequences of the southern Pyrenees. *Am. Ass. Petrol. Geol., Mediterranean Basins Conference* **7**.

Nyk, R. 1985. Illite crystallinity in Devonian slates of the Meggen mine (Rhenish Massif). *Neues Jb. Miner. Mh.* **1985**, 268–276.

Ori, G. G. & Friend, P. F. 1984. Sedimentary basins formed and carried piggyback on active thrust sheets. *Geology* **12**, 475–478.

Pique, A. 1982. Relations between stages of diagenetic and metamorphic evolution and the development of primary cleavage in the northwestern Moroccan Meseta. *J. Struct. Geol.* **4**, 491–500.

Plessman, W. 1965. Gesteinslösung, ein Hauptfaktor beim Schieferungsprozess. *Geologische Mitteilungen* **4**, 69–82.

Puigdefábregas, C. 1974. Les sédiments de marée du Basin Eocene Sudpyrenéen. *Bulletin de la Centre Recherches, Pau-SNPA*. **8**, 305–325.

Puigdefábregas, C. 1975. La sedimentatión molásica en la cuenca de Jaca. *Monographias del Instituto de Estudios Pirenaicos*. **104**.

Rossell, J. & Puigdefábregas, C., editors 1975. The sedimentary evolution of the Paleogene South Pyrenean Basin. I.A.S. International Congress, Nice, France.

Rowe, K. J. & Rutter E. H. 1990. Paleostress estimation using calcite twinning: experimental calibration an application to nature. *J. Struct. Geol.* **12**, 1–18.

Rutter, E. H. 1983. Pressure solution in nature, theory and experiment. *J. Geol. Soc. Lond.* **140**, 725–740.

Sibson, R. H. 1977. Fault rocks and fault mechanisms. *J. Geol. Soc. Lond.* **133**, 191–213.

Siddans, A. W. B. 1977. The development of slaty cleavage in a part of the French Alps. *Tectonophysics* **39**, 533–557.

Trurnit, P. 1968. Pressure solution phenomena in detrital rocks. *Sediment. Geol.* **2**, 89–114.

Tullis, T. E. 1980. The use of mechanical twinning in minerals as a measure of shear stress magnitudes. *J. geophys. Res.* **85**, 6263–6268.

Turner, F. J. 1953. Nature and dynamic interpretation of deformation lamellae in calcite of three marbles. *Am. J. Sci.* **251**, 276–298.

Van Hoorn, B. 1970. Sedimentology and paleogeography of an Upper Cretaceous turbidite basin in the south-central Pyrenees, Spain. *Leid. geol. Meded.* **45**, 73–154.

Wojtal, S. W. & Mitra, G. 1988. Nature of deformation in some fault rocks from Appalachian thrusts. In: *Geometries and Mechanics of Thrusting, With Special Reference to the Appalachians* (edited by Mitra, G. & Wojtal, W.). *Spec. Pap. geol. Soc. Am.* **222**, 17–33.